Published in final edited form as:
Bioconjug Chem. 2008 November 19; 19(11): 2221–2230. doi:10.1021/bc8003205.

Site-Selective Glycosylation of Hemoglobin on Cys β93

Yalong Zhang[a], **Veer S. Bhatt**[b], **Guoyong Sun**[c], **Peng G. Wang**[a,b], and **Andre F. Palmer**[c,*]

a*Department of Chemistry, The Ohio State University, Columbus, OH, 43210, U.S.A.*

b*Biophysics Program and Department of Biochemistry, The Ohio State University, Columbus, OH, 43210, U.S.A.*

c*Department of Chemical and Biomolecular Engineering, The Ohio State University, Columbus, OH, 43210, U.S.A.*

Abstract

In this work, we describe the synthesis and characterization of a novel glycosylated hemoglobin (Hb) with high oxygen affinity as a potential Hb-based oxygen carrier. Site-selective glycosylation of bovine Hb was achieved by conjugating a lactose derivative to Cys 93 on the β subunit of Hb. LC-MS analysis indicates that the reaction was quantitative, with no unmodified Hb present in the reaction product. The glycosylation site was identified by chymotrypsin digestion of the glycosylated bovine Hb followed with LC-MS/MS and from the X-ray crystal structure of the glycosylated Hb. The chemical conjugation of the lactose derivative at Cys β93 yields an oxygen carrier with a high oxygen affinity (P_{50} of 4.94 mmHg) and low cooperativity coefficient (n) of 1.20. Asymmetric flow field-flow fractionation (AFFFF) coupled with multi-angle static light scattering (MASLS) was used to measure the absolute molecular weight of the glycosylated Hb. AFFFF-MASLS analysis indicates that glycosylation of Hb significantly altered the $\alpha_2\beta_2$-$\alpha\beta$ equilibrium compared to native Hb. Subsequent X-ray analysis of the glycosylated Hb crystal showed that the covalently linked lactose derivative is sandwiched between the β_1 and α_2 (and hence by symmetry the β_2 and α_1) subunits of the tetramer, and the interaction between the saccharide and amino acid residues located at the interface is apparently stabilized by hydrogen bonding interactions. The resultant structural analysis of the glycosylated Hb helps to explain the shift in the $\alpha_2\beta_2$-$\alpha\beta$ equilibrium in terms of the hydrogen bonding interactions at the $\beta_1\alpha_2/\beta_2\alpha_1$ interface. Taken together, all of these results indicate that it is feasible to site-specifically glycosylate Hb. This work has great potential in developing an oxygen carrier with defined chemistry that can target oxygen delivery to low pO_2 tissues and organs.

INTRODUCTION

Hemorrhagic shock is a well-documented clinical condition in which 50% of the blood volume is lost due to some trauma. The loss of oxygen carrying capacity results in the development of low pO_2 levels in key organs like the brain, liver and heart. Therefore, it is imperative that resuscitation strategies first target oxygen delivery to these low pO_2 tissues and organs in order to preserve their function, before transporting oxygen to well oxygenated sites in the body (1). Since hemoglobin (Hb) is responsible for oxygen transport and storage in red blood cells (RBC), it is not surprising that much effort has been spent to develop hemoglobin-based oxygen carriers (HBOCs) for treatment of hemorrhagic shock. The initial development of RBC substitutes was driven by the needs of the military (2). Early attempts towards developing a RBC substitute using acellular Hb in human recipients met with failure due to hypertension,

*To whom correspondence should be addressed. Department of Chemical and Biomolecular Engineering, The Ohio State University, 231A Koffolt Laboratories, 140 West 19th Avenue, Columbus, Ohio 43210, Tel: (614) 292-6033 and E-mail: E-mail: palmer.351@osu.edu.

short intravascular half-life and nephrotoxicity (3). These problems have been attributed in large part to the affinity of Hb for nitric oxide (4). and dissociation of the $\alpha_2\beta_2$ tetramer into αβ dimers that can further unfold to release cytotoxic heme that is eventually filtered through the renal glomeruli (2,5–7).

In order to overcome the disadvantages associated with transfusing acellular Hb, several types of HBOCs have been developed over the past 20 years, such as: cross-linked Hb (8–10), polymerized Hb (6,11–14), surface conjugated Hb (15–19), liposome (20–24) and nanoparticle encapsulated Hb (25–27), and recombinant Hb (7,28,29).

In nature, glycoproteins possess a large hydration shield afforded by relatively small oligosaccharides (30), which will protect a protein from proteolysis and stabilize the protein by forming hydrogen bonds with amino acid residues on the protein surface. Glycosylation of Hb at Lys or *N*-terminal amines in the systemic circulation by glucose is a well known reaction (31,32). Previously, oxidized dextran (10,33) and oxidized raffinose (Hemolink™, Hemosol Inc., Toronto, Canada) (33–35) were used to cross-link and polymerize Hb in order to increase its molecular radius and to prevent its extravasation through blood vessels by modification of amine groups on proteins. However, those early attempts at cross-linking and polymerizing Hb with oxidized saccharides yielded highly heterogeneous products with the resultant chemical modification of key amino acid residues that regulate oxygen affinity and the structural stability of the tetramer. In the case of Hemolink™, Alayash et al. (36) confirmed that *O*-raffinose cross-linked and polymerized Hb were constrained in a locked T-state conformation that promotes heme instability. In addition, *in vivo* experiments also showed that Hemolink™ induces microvascular damage and increases the permeability of the microvasculature when compared to other HBOCs (37). In light of these results, recent advances in glycochemistry indicate that it is important and necessary to prepare homogenous glycoproteins with specific glycosylation sites (38).

In the present study, the feasibility of site-selective glycosylation of bovine Hb (Figure 1) was investigated by conjugating a reactive lactose derivative to Cys β93. Bovine Hb was chosen as the source of Hb, since it has two cysteine residues per tetramer, each located at the Cys 93 position on the β subunit. Conversely, human Hb has 6 cysteine residues. Cys β93 is located in a conformationally plastic domain, which contains amino acid residues that regulate the allosteric properties of the Hb tetramer (39). Previous modification of Cys β93 with maleimide resulted in an increase in oxygen affinity and the loss of some hydrogen bonds within the $\alpha_1\beta_2/\alpha_2\beta_1$ interface of Hb (39–41). In this study, the modified lactoside derivative could compensate for the lost hydrogen bonds by forming additional hydrogen bonds with amino acid residues within the $\alpha_1\beta_2/\alpha_2\beta_1$ interface in order to stabilize the tetrameric structure of Hb as well as to increase the molecular radius of Hb, therefore facilitating in preventing its extravasation through the lumen of blood vessels and subsequent NO scavenging.

EXPERIMENTAL PROCEDURES

Materials

β-D-Lactose, 2-[2-(2-chloroethoxy)ethoxy]ethanol, and 6-maleimidohexanoic acid *N*-hydroxysuccinimide ester were purchased from Sigma-Aldrich (Milwaukee, WI) and used without further purification. HEMOX-solution, additive-A, and anti-foaming agent were purchased from TCS Scientific Corp. (New Hope, PA). Bovine RBCs were purchased from QUAD 5 (Ryegate, MT). All other reagents, unless specified, were obtained from commercial sources and used without further purification. Solvents were distilled from the appropriate drying agents before use. Unless stated otherwise, all reactions were carried out at room temperature under a positive pressure of argon or nitrogen and were monitored by TLC on silica gel 60 F254 (0.25 mm, E. Merck, Gibbstown, NJ). Spots were detected under UV light

or by anisole anhydride/H_2SO_4/MeOH (5/15/80). Column chromatography was performed on silica gel 60 (230–400 mesh) purchased from EMD Chemicals Inc. (Darmstadt, Germany). The ratio between silica gel and crude product ranged from 20 to 30:1 (w/w). For the characterization of reaction products, ^{1}H NMR spectra were recorded at 500 MHz, and chemical shifts referenced to $CDCl_3$ (7.26, $CDCl_3$). ^{13}C NMR spectra were recorded at 125 MHz, and ^{13}C chemical shifts referenced to $CDCl_3$ (77.00, $CDCl_3$).

Synthesis of *N*-3',6'-dioxa-9'-octyl-*O*-(β-D-glucopyranolsyl)-(1→4)-β-D-galactoside-6-maleimidohexanamide (maleimide-lactoside)

The method of preparing maleimide-lactoside is shown in Scheme 1. First, the peracetyl protected lactoside **1** was treated with 2-[2-(2-chloroethoxy)ethoxy]ethanol catalyzed by boron trifluoride and then reacted with sodium azide to yield 1-azido-4,6-dioxa-9-octyl-peracetyl-lactoside **2**. Second, the acetyl groups were removed by treating with sodium methoxide to yield compound **3**. Finally, the azido group of **3** was hydrogenated to an amine and reacted with 6-maleimidohexanoic acid *N*-hydroxysuccinimide ester to yield maleimide-lactoside **4**.

Hb Purification (42,43)

Hb was extracted from bovine RBCs suspended in 3.8% sodium citrate solution. RBCs were washed 3 times with 3 volumes of isotonic saline solution (0.9%) at 4 °C. Cells were then lysed with 2 volumes of hypotonic, 15 mOsM phosphate buffer (PB), pH 7.4 on ice for 1 h. Lysed cells were then filtered 3 times through glass wool and a filter paper to remove cell debris. The crude solution of Hb was dialyzed against 20 mM Tris-HCl buffer (pH=8.2). This buffer was the starting buffer for the chromatographic purification of Hb. Hb purification was performed using an ÄKTA Explorer 100 system controlled by Unicorn 5.1 software (GE Healthcare, Piscataway, NJ). Dialyzed Hb lysate was loaded onto a XK 26/40 (400 mm in length and 26 mm I.D., GE Healthcare, Piscataway, NJ) column packed with 120 mL Q-Sepharose XL resin (GE Healthcare, Piscataway, NJ) and eluted with a linear salt gradient (0 to 0.15 M NaCl in 5 column volumes). The eluted Hb was collected with a fraction collector (Frac 900, GE healthcare, Piscataway, NJ). The purity of Hb was assessed by SDS-PAGE. Pure Hb fractions were pooled for measurement of Hb concentration and methemoglobin (metHb) level. The concentration of Hb and metHb in solution was determined using an adaptation of the cyanomethemoglobin (cyanometHb) method (20,44). Hb solution was placed in a 1.5 mL cuvette and diluted with buffer (20 mM PB, pH 7.2) with a total volume of 1.0 mL (dilution factor: D_1) in order to yield an absorbance less than 1 at 630 nm (oxyHb+deoxyHb+metHb). Potassium cyanide (KCN) solution (50 μL, 10% KCN in 50 mM PB, pH 7.6) was added to the solution to convert metHb into cyanometHb and the absorbance was measured at 630 nm to yield L_2 (since cyanometHb does not absorb at 630 nm), L_2 refers to the absorbance of oxyHb +deoxyHb. Thus the concentration of metHb can be obtained from this equation: [metHb] = $D_1(L_1-L_2)/3.7$ mM. To measure the concentration of Hb, potassium ferricyanide ($K_3Fe(CN)_6$) (50 μL, 20% $K_3Fe(CN)_6$ in 50 mM PB, pH 7.6) was mixed with diluted Hb solution (dilution factor: D_2), which converts oxyHb and deoxyHb into metHb. The solution was incubated for 5 min and then KCN (50 μL, 10% KCN in 50 mM PB, pH 7.6) was added to the mixture to convert metHb to cyanometHb. The absorbance was measured at 540 nm (L_3). Thus [Hb] = $D_2L_3/11$ mM.

Site-Selective Glycosylation of Hb

To a solution of Hb (60 mg, 9.34×10^{-4} mmol) in Tris-HCl buffer (20 mM, pH 8.2, 2.0 mL) was added maleimide-lactoside **4** (4.4 mg, 6.56×10^{-3} mmol) which was stirred at r.t. for 24 h. Sodium cyanoborohydride (12 mg, 9.34×10^{-2} mmol) was added to the reaction mixture and the solution was stirred for another 24 h. The modified Hb was transferred to a Millipore centrifugal filter device (10,000 MW cutoff) and washed 4 times with Tris-HCl buffer (20 mM,

pH 8.2, 2.0 mL) in a centrifuge at 5000 rpm to remove unreacted maleimide-lactoside **4** and sodium cyanoborohydride.

Analysis of Glycosylated Hb by LC-MS

LC-MS analysis of purified Hb and glycosylated Hb was performed on a Waters Alliance 2690 high-performance liquid chromatography (HPLC) system (Waters, Milford, MA) connected in series to a Waters LCT (Waters, Milford, MA) mass detector. Samples were analyzed using a Vydac C18 column (5 μm particle size, 1.0 × 250 mm) at a flow rate of 50 μL/min and injection volume of 10 μL. The mobile phase consisted of the following: phase A, 0.1 % trifluoroacetic acid, and phase B, acetonitrile/0.1% trifluoroacetic acid. The percentage of phase B was increased according to a linear gradient from 0 to 65 % in 45 min and then increased from 65 to 100% in 15 min. The amino acid sequence and molecular weight of bovine Hb was obtained from ProteinProspector at UCSF (http://prospector.ucsf.edu/).

Chymotrypsin Digestion of the β Chain of Glycosylated Hb

The β chain of glycosylated bovine Hb was purified via a Shimadzu HPLC LC-20AT (Columbia, MD) equipped with a Supelco bio wide pore C18 column (5 μm in particle size, 15×150 mm, and 300 Å in pore size, Sigma-Aldrich, Milwaukee, WI). The mobile phase and gradient were the same as those utilized in the LC-MS analysis. 20 μL of glycosylated bovine Hb (15 mg/mL) was injected into the RP-HPLC column and the second peak was collected (22.67 min). The molecular weight of the collected fraction was confirmed by LC-MS 2010A (Shimadzu, Columbia, MD). The lyophilized protein was digested using a protocol similar to the reference (45) at the Campus Chemical Instrument Center (CCIC) at The Ohio State University by Dr. Liwen Zhang. Proteins were desalted using manual syringe protein traps from Michrom BioResources (Auburn, CA) and re-suspended in 10 μL of water. 5 μL of DTT (5 mg/mL) in 100 mM ammonium bicarbonate was incubated with the sample at 50 °C for 15 min to reduce all cysteine residues. 5 μL of iodoacetamide (15 mg/mL) in 100 mM ammonium bicarbonate was then added and incubated with the mixture in the dark for 15 min to alkylate the cysteine residues. Sequencing grade chymotrypsin from Roche was prepared as 25 ng/μL in 50 mM ammonium bicarbonate. The final buffer conditions for digestion were 25 mM ammonium bicarbonate and 5% acetonitrile. The digestion was carried out at 37 °C overnight and terminated by acidification. The digest was concentrated in a speed vac to ~30 μL for subsequent LC-MS/MS analysis.

LC-MS/MS Analysis of the β Chain of Glycosylated Hb

Capillary-liquid chromatography-nanospray tandem mass spectrometry (LC-MS/MS) was performed on a Thermo Finnigan LTQ mass spectrometer equipped with a nanospray source operated in positive ion mode at CCIC by Dr. Liwen Zhang. The LC system was an UltiMate™ Plus system from LC-Packings (Sunnyvale, CA) with a Famos autosampler and a Switchos column switcher. 5 μL of each sample was first injected into the trapping column (LC-Packings), and washed with 50 mM acetic acid. The injector port was switched to inject, and the peptides were eluted off the trap onto a 5 cm, 75 μm (inner diameter) ProteoPep II C18 reverse-phase column (New Objective, Inc. Woburn, MA) packed directly in the nanospray tip. Solvent A was composed of 50 mM acetic acid in water and solvent B was composed of acetonitrile. Peptides were eluted directly off the column into the LTQ system at a flow rate of 300 nL/min. The gradient was initiated and maintained at 2% B for the first 3 min, then B was increased to 50% in 27 min, and further increased to 80% in 15 min. B was kept at 80% for another 5 min, then returned to 2% in 0.1 min. The total run time was ~ 65 min.

The MS/MS was acquired according to the standard conditions established at the CCIC. Briefly, a nanospray source operating at a spray voltage of 3 KV and a capillary temperature of 200°C was used. The scan sequence of the mass spectrometer was based on the TopTen™

method, briefly the analysis was programmed for a full scan to be recorded between 350–2000 Da, and a MS/MS scan was used to generate product ion spectra to determine the amino acid sequence in consecutive instrument scans of the ten most abundant peaks in the spectrum. The CID fragmentation energy was set to 35%. Dynamic exclusion was enabled with a repeat count of 30 seconds, exclusion duration of 350 seconds and a low mass width of 0.5 and high mass width of 1.5 Da. Sequence information from the MS/MS data was processed using the Mascot 2.0 active Perl script with standard data processing parameters. The data was later searched by MASCOT 2.0 (Matrix Science, Boston, MA) for protein identification and MassMatrix for the identification of cysteine glycosylation (46). Methionine oxidation and carbamidomethylation of cysteines were also considered as possible modifications.

Crystallization of Glycosylated Hb

Purified glycosylated Hb was used for all crystallization experiments. The protein was concentrated to 30 mg/mL in Tris-HCl Buffer (20 mM, pH 7.4), and a microbatch experiment was set up (47) under mineral oil (Sigma-Aldrich) at 25°C. To find initial crystallization hits, sample drops were set-up against commercial (Hampton Research, CA) as well as home made screens in a ratio of 1:2. Crystalline forms could be observed in several different precipitants in the pH range 7.5–8.5. These conditions were optimized further by varying the concentration and pH of the corresponding crystallization reagent for each hit. Eventually, crystals grown in reagent droplets containing 25% w/v PEG MME 2000, 0.2 M Trimethylamine *N*-oxide dehydrate and 0.1 M Tris pH 8.25 were used to collect full datasets. These crystals grew as clustered thin plates with the longest dimension measuring 100 μm. They were flash frozen after cryoprotection using 38% PEG MME 2000 and stored in liquid nitrogen until further use.

Data Collection and Processing

The X-ray intensity data to 3.5 Å resolution was collected at −160 °C using a R-AXIS IV++ imaging plate area detector and Cu K radiation generated from a rotating-anode X-ray generator (Rigaku-MSC, TX) operating at 46 kV and 90 mA. The temperature was maintained during data collection using an X-STREAM cryogenic device (Rigaku-MSC, TX). Although crystals diffracted to 3.3 Å, the completeness beyond 3.5 Å was lower than 20%. Therefore, the final data set was collected to 3.5 Å resolution. The data were processed using the CrystalClear software which is based on the d*TREK package (48). The crystals belong to the orthorhombic space group $P2_12_12_1$ with one molecule in the asymmetric unit. The unit-cell parameters are $a = 62.6$, $b = 74.0$ and $c = 129.8$ Å. Solvent analysis suggested only one molecule to be present in the asymmetric unit. Assuming that one protein molecule in the asymmetric unit has a molecular weight of 64 kDa, V_M was calculated to be 2.35 $Å^3Da^{-1}$. The details of the crystallographic data are summarized in Table 1 in supporting information.

Structure Determination and Refinement

The structure of bovine Hb is already well known (46). However, the protein can exist in different quaternary states depending on whether it is liganded (R-state) or not (T-state). Furthermore, several intermediate quaternary forms have been found to exist and is apparently governed by pH (49). Thus, structure determination could be pursued by molecular replacement (49,50) only when the correct quaternary model was provided. In doing so, three starting models of carbonmonoxy bound Hb (48) with p.d.b. ids 1g0a, 1g08 and 1g09 were evaluated. 1g0a clearly gave the best solution among all the models (R-factor: 37.0 % and correlation coefficient: 70.5 %). Crystals of model (1g0a) were also grown at a pH (8.5) similar to that of our sample protein (8.25) further corroborating its validity as the correct model.

The model obtained from molecular replacement was refined using the program REFMAC (51). The initial steps of manual model building with the program coot (52) using $|2F_o - F_c|$ and $|F_o - F_c|$ Fourier maps yielded R and R_{free} factors of 0.322 and 0.357, respectively. Densities

of the lactose and its succinimide linker were clearly evident (Figure 5) in the vicinity of Cys93 of the β subunit of the protein. Densities for all four bound heme groups and Fe^{3+} were clearly observed at this stage. The model thus obtained including the sugar and co-factors was subjected to several cycles of refinement alternating with several rounds of manual model building. Although the positions of water molecules were not sought at this resolution, there were good densities in $|2F_o - F_c|$ and $|F_o - F_c|$ for 8 water molecules which seemed to hydrogen bond with various protein atoms. These were therefore included in the further refinement, to which they responded well. The R and R_{free} factors finally converged to 0.268 and 0.332, respectively. The refinement statistics are given in Table 2 (available in supporting information) (53,54). The program PROCHECK was used to validate the quality of the final structure (54). 91.1% of the residues were found in the most favored regions of the Ramachandran plot (55) and the remaining residues were in the additionally allowed regions.

Quality of the Model

The final coordinate set consists of 4582 non-hydrogen atoms from a total of 574 amino acid residues, one sugar-moiety covalently bound to Cys93 (on the β_1 subunit) via a succinimide linkage, four heme groups each with Fe^{3+} coordinated in the center and two water molecules. The electron density map of the second sugar molecule was not as discernible, given the highly flexible nature of the linker. Thus only one sugar molecule was incorporated in the final coordinate set. The protein structure exhibited a geometry close to ideal values, with root mean square (r.m.s.) deviations of 0.006 Å and 1.01 Å from standard values of bond lengths and bond angles, respectively. The overall mean B factor was found to be 91.2 $Å^2$. The high value of the B factors suggests that the quality of glycosylated Hb crystals is not good. Despite this, the electron density was very well defined for almost all of the main-chain of the protein, all the heme groups and even one of the covalently bound lactoses.

Oxygen Equilibria of Glycosylated Hb

Oxygen equilibrium curves of native Hb/glycosylated Hb were measured on a Hemox analyzer (TCS Scientific, New Hope, PA). This instrument simultaneously measures the Hb saturation via dual-wavelength spectrophotometry, while measuring the dissolved oxygen concentration with a Clark oxygen electrode. The temperature was maintained at 37 °C for all measurements. Samples were prepared by thoroughly mixing 500 μL of native Hb or glycosylated Hb with 5 mL of the Hemox buffer (pH 7.4, TCS Instruments, Southampton, PA), 20 μL of Additive-A, 10 μL Additive-B and 10 μL of anti-foaming agent. The sample was saturated with compressed air at a pO_2 of 145±2 mmHg. Then the gas stream was switched to pure N_2 to deoxygenate the sample. The absorbance of oxy- and deoxy-Hb in solution was recorded as a function of pO_2 via dual wavelength spectroscopy. Oxygen equilibrium curves were fit to a four-parameter (A_0, A_∞, P_{50}, n) Hill model (Equation 1). In this model, the P_{50} represents the pO_2 at which Hb is half saturated with O_2, n is the Hill coefficient, while A_0 and A_∞, represent the absorbance at 0 mmHg and full saturation, respectively.

$$Y = \frac{Abs - A_0}{A_\infty - A_0} = \frac{pO_2^n}{pO_2^n + P_{50}^n} \qquad \text{(Equation 1)}$$

Molecular Weight Distribution Analysis of Glycosylated Hb

An asymmetric flow field-flow fractionator (AFFFF) (Wyatt Technology Corp., Santa Barbara, CA) coupled in series with a multi-angle static light-scattering (MASLS) photometer (Wyatt Technology Corp.) and a differential interferometric refractometer (DIR) (Wyatt Technology Corp) was used to measure the absolute molecular weight distribution of native Hb and glycosylated Hb. During a typical experiment, the sample is injected into the AFFFF channel,

where it is separated. The resultant eluent is then sent through the flow cell of the MASLS photometer, which continuously measures the macromolecule's Raleigh ratio (scattered light intensity) at 16 angles. The eluent is then sent through the flow cell of the DIR, which measures the macromolecule's concentration. Using a formulation of the angular distribution of scattered light derived by Zimm, it is possible to extract the molecular weight of each eluting monodisperse slice of the fraction (56). Hence, we can measure the absolute molecular weight of native and glycosylated Hb to evaluate whether glycosylation still favors the tetrameric structure of native Hb. All measurements were conducted at 25 °C. In preparation for AFFFF-MASLS-DIR experiments, all glassware was carefully cleaned, and all solutions were thoroughly filtered through 0.2 μm filters.

AFFFF-MASLS-DIR measures the weight average molecular weight (M_w) of native and glycosylated Hb in solution. M_w is defined as:

$$M_w = \frac{\sum_i (c_i M_i)}{\sum_i c_i} \quad \text{(Equation 2)}$$

Where c_i is the mass concentration of component *i* in solution, and M_i is the molecular weight of component *i* in solution. In solution, the Hb tetramer will exist in equilibrium with αβ dimers. Therefore, if C_T is the total mass concentration of Hb in the tetrameric and dimeric forms, then we can write expressions for the mass concentration of tetramer ($C_{\alpha 2\beta 2}$) and dimer ($C_{\alpha\beta}$) in solution if $x_{\alpha\beta}$ represents the mass fraction of αβ dimers in solution.

$$C_{\alpha\beta} = C_T x_{\alpha\beta} \quad \text{(Equation 3)}$$

$$C_{\alpha 2\beta 2} = C_T (1 - x_{\alpha\beta}) \quad \text{(Equation 4)}$$

Substituting equations 3 & 4 into equation 2 yields an expression for $x_{\alpha\beta}$ (Equation 5).

$$x_{\alpha\beta} = \frac{M_w - M_{\alpha 2\beta 2}}{M_{\alpha\beta} - M_{\alpha 2\beta 2}} \quad \text{(Equation 5)}$$

Hence, M_W (measured with AFFFF-MASLS-DIR), $M_{\alpha 2\beta 2}$(theoretical mass of tetrameric Hb) and $M_{\alpha\beta}$ (theoretical mass of dimeric Hb) and substituting these parameters into equation 5 allows us to calculate $x_{\alpha\beta}$ and thus the mass fraction of tetrameric Hb ($x_{\alpha 2\beta 2} = 1 - x_{\alpha\beta}$).

RESULTS AND DISCUSSION

Preparation of Glycosylated Bovine Hb

Bovine Hb is a tetramer, which consists of two identical α chains and two identical β chains. The amino acid sequence of bovine Hb shows that only one cysteine, Cys-93, is located on the β chain. The molecular weight of the α chain and β chain are 15053 and 15955 Da respectively. Since maleimide-lactoside **4** (M_w = 666 Da) can selectively react with thiol groups on cysteine residues, the reactive disaccharides can be selectively conjugated to Cys-93 on the β chain. As a result, the molecular weight of the β chain increases to 16621 Da. In order to verify the

glycosylation of bovine Hb by maleimide-lactoside **4**, the mass spectra of native bovine Hb and glycosylated Hb was measured by LC-MS (Figure 2 and Figure 3, respectively).

In Figure 2, only two peaks were present in the RP-HPLC chromatogram (graph A). The ESI mass spectrum of the first peak (graph B) was deconvoluted to yield the mass of the molecular ion, 15054 Da (graph C), which indicates that the first peak was due to the α chain of bovine Hb. The ESI mass spectrum of the second peak (graph D) was deconvoluted to yield the mass of the molecular ion, 15955 Da (graph E), which indicates that the second peak was due to the β chain of bovine Hb. Comparing native bovine Hb (Figure 2) and glycosylated Hb (Figure 3), there was no significant difference in the retention time for both peaks in the LC chromatograms. Since it is the polarity of the molecule that determines the retention time in reverse phase chromatography, this result indicates that the polarity of glycosylated Hb was not changed. The molecular weight of the α chain of the glycosylated Hb was 15054 Da (Figure 3C), which was calculated by deconvolution of the ESI mass spectrum (Figure 3B). This result indicates that no lactoside derivative was conjugated to the α chain. However, the ESI mass spectrum of the second peak of Figure 3 (graph D) when deconvoluted (graph E) showed that the molecular weight of the β chain of glycosylated Hb increased to 16622 Da. Therefore, the molecular weight difference between the β chain of natural Hb and glycosylated Hb is 667 Da, which is consistent with the molecular weight of maleimide-lactoside **4** (M_w = 666.3 Da). Therefore LC-MS analysis of glycosylated Hb indicates that maleimide-lactoside is conjugated only to the β chain of Hb. Furthermore, the absence of a mass peak at 15955 Da in graph E implies the absence of any unmodified β chains. This result shows that the conjugation reaction was quantitative and required no separation of unreacted protein products.

Determination of the Glycosylation Site on Bovine Hb

Tandem mass spectrometry was performed on the peptide fragments derived from the β chain of glycosylated bovine Hb digested by chymotrypsin, which will cleave the protein at Phe, Tyr and Trp (57). The resulting data permits us to identify the conjugated latoside derivative, the chemotryptic peptides (AALSELHC*DKLHVDPENF) ($T_{\beta 85–102}$) and the glycosylation site in Figure 4 (The proteolytic MS-MS data are available in the supporting information section). The calculated molecular weight for the glycosylated $T_{\beta 85–102}$ was 2704.3 Da. Peaks at 1271.56 (2+) and 848.08 (3+) were observed, which translate into molecular weights of 2542.12 Da and 2542.24 Da respectively. The difference between the calculated molecular weight and the observed data was 162, which corresponds to the loss of one hexose. Peaks at 1190.84 (2+) and 794.50 (3+) were also observed, which correspond to a molecular weight 324 Da less than the calculated data (two hexoses lost). These observations confirm the conjugation of the lactoside derivative (a disaccharide) on this peptide fragment. Secondly, the peptide sequence were confirmed by observation of the ion series from b13 to b17, showing the loss of the DPENF sequence from the peptide fragment. Finally, the observation of y13 (1117.72^{2+}), y9 (550.32^{2+}) and b6 (585.03) indicate that the modified amino acid was located on the three peptide sequence HCD.

X-ray Structure of Glycosylated Hb

The complete amino-acid sequence of bovine Hb shows that both α subunits consist of 141 and both β subunits consist of 145 amino acid residues. A sequence comparison with human Hb performed using CLUSTALW (58) shows 88% sequence identity in the α and 84% sequence identity in the β subunits. Thus, it is apparent that bovine Hb can serve as a good functional and structural mimic of human Hb.

It was found that the homogenous lactoside glycosylated Hb can be crystallized and the crystal was analyzed to verify the site of modification and to access any structural changes associated with the glycosylation reaction. The crystal structure could provide definitive evidence that

the Hb is glycosylated (Figure 5 and Figure 6). The electron density of one succinimide linked lactose could be found with slight discontinuity close to Cys β93 at 0.7σ cutoff in these maps. This result confirms the covalent glycosylation of the lactoside derivative at Cys β93. Since a significant deviation from native quaternary structure could strongly indicate a loss in function, this possibility had to be investigated. It was found that the structure of glycosylated bovine Hb was very similar to native bovine Hb (Figure 7). The overall r.m.s. deviation between the two structures was found to be as low as 0.40 Å. The overall quaternary fold is essentially identical to the native protein (p.d.b. id 1g0a) in most parts of the superimposition as seen in Figure 7. The only parts where there are discernible albeit minor differences in the fold are the two surface loops and the two glycosylation sites (red) compared with that of native Hb (blue). Since the Cys β93 residue forming the glycosylation site is part of a helix, this imposes severe geometrical constraints on it, and thus, probably prevents it from distorting the overall tertiary fold. The disturbance in the tertiary structure by chemical modification results in the breakage of the β94-β146 and β146-α40 hydrogen bonds (39–41). This lost of hydrogen bonds will help to destabilize the T-state (40) and increase the oxygen binding affinity as well as decrease the cooperativity.

Oxygen Equilibria of Glycosylated Hb

The oxygen dissociation curves are shown in Figure 8 for native and glycosylated Hb. For native Hb, the P_{50} is 26.44 torr while for glycosylated Hb it is only 4.94 torr. The P_{50} is an indicator of oxygen affinity, and refers to the partial pressure of oxygen at which half of the HBOC is saturated with oxygen. The low P_{50} of the glycosylated Hb indicates that it has a higher affinity for oxygen versus native Hb. Furthermore, it was found that the cooperativity coefficient of glycosylated Hb is 1.2, which is almost half compared with that of native Hb (2.23). The cooperativity of hemoglobin is associated with the allosteric transition from T-state (tense) to R-State (relaxed) upon oxygenation (39). One reason for the decrease in cooperativity can be explained by the disturbance of the tertiary structure of Hb by maleimide modification of Cys β93. Another reason may be due to structural changes imposed by the glycosylation reaction. Based on the crystal structure (Figure 6), it was found that the lactose derivative is located within the $\alpha_1\beta_2/\alpha_2\beta_1$ interface. As a result, the additional hydrogen bonds between the disaccharide and various amino acid residues within the interface will hinder the transition from T-state to R-state and thus leads to a decrease in cooperativity. On the other hand, the additional hydrogen bonding interactions between the disaccharide and various amino acid residues at the interface could stabilize the overall tetrameric structure of Hb. This would be a novel feature of the glycosylated Hb and indicates that it should be more stable (not dissociate into αβ dimers) in the blood stream versus native Hb when transfused into patients. In addition, the high oxygen affinity of the glycosylated Hb indicates that it can be used to treat hemorrhagic shock by delivering oxygen to regions of the body with low oxygen levels instead of systemically.

AFFFF-MASLS-DIR of Glycosylated Hb

In order to prove our hypothesis that glycosylation of Hb will stabilize the tetrameric structure of Hb, an asymmetric flow field-flow fractionator (AFFFF) coupled in series with a multi-angle static light-scattering (MASLS) photometer was used to measure the absolute molecular weight distribution of native Hb and glycosylated Hb. In aqueous solution, the Hb tetramer ($\alpha_2\beta_2$) exists in equilibrium with αβ dimers. Because of this equilibrium, the measured molar mass of Hb in solution will be between that of the intact $\alpha_2\beta_2$ tetramer (64 kDa) and the αβ dimer (32 kDa). In Figure 9, we observe this behavior. The average M_w for native Hb was calculated to be 53.5 kDa and was 58.3 kDa for glycosylated Hb. The molecular weight of the native Hb tetramer and dimer is 64 kDa and 32 kDa, respectively. If two lactose derivatives are conjugated to the native Hb tetramer, the resultant molecular weight of the glycosylated Hb tetramer and dimer are 65.334 kDa and 32.667 kDa, respectively. Therefore, substituting

these values into equation 5 reveals that the mass fraction of $\alpha_2\beta_2$ is 0.67 for native Hb in solution, and 0.78 for glycosylated Hb, respectively. Hence, the increase in the mass fraction of $\alpha_2\beta_2$ tetramer for glycosylated Hb indicates that the $\alpha_1\beta_2$ /$\alpha_2\beta_1$ interface between adjacent αβ dimers is more "sticky" for glycosylated Hb versus native Hb. The origin of this "stickyness" can be elucidated by recognizing that the sugar is sandwiched between the β_1 and α_2 subunits of the protein (Figure 6). Interestingly, hydrogen bonds are formed between the sugar molecule and amino acid residues within the $\alpha_2\beta_1$ interface, and it is this hydrogen bonding interaction that leads to the "stickyness" of the αβ interface by stabilizing the overall tetrameric structure of Hb. This observation further explains why the equilibrium of glycosylated Hb favors the tetrameric structure when compared to native Hb. Therefore, an added benefit of the glycosylation reaction is that it can stabilize the tetrameric structure of Hb. As mentioned earlier, this feature will reduce the formation of αβ dimers and therefore reduce the amount of Hb extravasation through the lumen of blood vessels and subsequent NO scavenging.

CONCLUSION

We describe in this work an approach for the site-selective chemical glycosylation of Hb as a potential HBOC. A lactoside derivative with a terminal maleimide moiety was synthesized and conjugated to Cys 93 on the β chain of bovine Hb. The glycosylation reaction was quantitative and required no special purification steps, which was confirmed by LC-MS. Chymotryptic digestion of the glycosylated β-globin chain followed by tandem mass spectroscopy and x-ray crystallography of the glycosylated Hb identified the glycosylation site at Cys β93. The glycosylation of Cys β93 on Hb results in an oxygen carrier with a high oxygen affinity (P_{50} = 4.94 mmHg) and low cooperativity coefficient (1.20). The stability of the glycosylated Hb was evaluated by AFFFF-MASLS-DIR analysis. AFFFF-MASLS-DIR analysis showed that the tetrameric structure of glycosylated Hb was more stable compared to native Hb. Subsequent x-ray analysis of the glycosylated Hb crystal revealed that the lactose derivative is sandwiched between the β_1 and α_2 subunits of the protein. This indicates that the glycosylated Hb is stabilized by hydrogen bonding interactions between the disaccharide and amino acids within the interface. These hydrogen bonding interactions explain the stability of the glycosylated Hb versus native Hb. In conclusion, glycosylated Hb exhibits high oxygen affinity and improved tetrameric stability, which shows great potential as an artificial blood substitute.

Supplementary Material

Refer to Web version on PubMed Central for supplementary material.

ACKNOWLEDGMENT

A. F. P. acknowledges the support of National Institutes of Health grants R01HL078840 and R01DK070862. P. G. W. acknowledges the support of National Institutes of Health grants U54NSO5818301

LITERATURE CITED

1. Mackenzie CF. Hemoglobin-based oxygen-carrying solutions and hemorrhagic shock. Semin. Anesth 2001;20:71–77.
2. Reid TJ. Hb-based oxygen carriers: are we there yet? Transfusion 2003;43:280–287. [PubMed: 12559026]
3. Rabiner SF, O'Brien K, Peskin GW, Friedman LH. Further studies with stroma-free hemoglobin solution. Ann. Surg 1970;171:615–622. [PubMed: 5436128]
4. Palmer AF. Molecular volume and HBOC-induced vasoconstriction. Blood 2006;108:3231–3232.
5. Chang TMS. Blood substitutes based on nanobiotechnology. Trends Biotechnol 2006;24:372–377. [PubMed: 16815577]

6. Haney CR, Buehler PW, Gulati A. Purification and chemical modifications of hemoglobin in developing hemoglobin based oxygen carriers. Adv. Drug Deliv. Rev 2000;40:153–169. [PubMed: 10837787]
7. Chang TMS. Hemoglobin-based red blood cell substitutes. Artif. Organs 2004;28:789–794. [PubMed: 15320941]
8. Hu T, Manjula BN, Li D, Brenowitz M, Acharya SA. Influence of intramolecular cross-links on the molecular, structural and functional properties of PEGylated haemoglobin. Biochem. J 2007;402:143–151. [PubMed: 17049048]
9. Vuletich DA, Falzone CJ, Lecomte, Juliette TJ. Structural and dynamic repercussions of heme binding and heme-protein cross-linking in Synechococcus sp. PCC 7002 hemoglobin. Biochemistry 2006;45:14075–14084. [PubMed: 17115702]
10. Eike JH, Palmer AF. Oxidized mono-, di-, tri-, and polysaccharides as potential hemoglobin cross-linking reagents for the synthesis of high oxygen affinity artificial blood substitutes. Biotechnol. Prog 2004;20:953–962. [PubMed: 15176904]
11. Eike JH, Palmer AF. Effect of Cl^- and H^+ on the oxygen binding properties of glutaraldehyde-polymerized bovine hemoglobin-based blood substitutes. Biotechnol. Prog 2004;20:1543–1549. [PubMed: 15458341]
12. Eike JH, Palmer AF. Effect of glutaraldehyde concentration on the physical properties of polymerized hemoglobin-based oxygen carriers. Biotechnol. Prog 2004;20:1225–1232. [PubMed: 15296452]
13. Eike JH, Palmer AF. Effect of $NaBH_4$ concentration and reaction time on physical properties of glutaraldehyde-polymerized hemoglobin. Biotechnol. Prog 2004;20:946–952. [PubMed: 15176903]
14. Dimino ML, Palmer AF. High O_2 affinity hemoglobin-based oxygen carriers synthesized via polymerization of hemoglobin with ring-opened 2-chloroethyl-β-D-fructopyranoside and 1-*O*-octyl-β-D-glucopyranoside. Biotechnol. Bioeng 2007;97:462–472. [PubMed: 17115452]
15. Jia Y, Ramasamy S, Wood F, Alayash AI, Rifkind JM. Cross-linking with *O*-raffinose lowers oxygen affinity and stabilizes haemoglobin in a non-cooperative T-state conformation. Biochem. J 2005;384:367–375. [PubMed: 15303971]
16. Nacharaju P, Manjula BN, Acharya SA. Thiolation mediated pegylation platform to generate functional universal red blood cells. Artif. Cells, Blood Substitutes, Biotechnol 2007;35:107–118.
17. Acharya SA, Acharya VN, Kanika ND, Tsai AG, Intaglietta M, Manjula BN. Non-hypertensive tetraPEGylated canine hemoglobin: correlation between PEGylation, O_2 affinity and tissue oxygenation. Biochem. J 2007;405:503–511. [PubMed: 17425516]
18. Li D, Manjula BN, Acharya AS. Extension arm facilitated PEGylation of hemoglobin: correlation of the properties with the extent of PEGylation. Protein J 2006;25:263–274. [PubMed: 16718519]
19. Hu T, Prabhakaran M, Acharya SA, Manjula BN. Influence of the chemistry of conjugation of poly (ethylene glycol) to Hb on the oxygen-binding and solution properties of the PEG-Hb conjugate. Biochem. J 2005;392:555–564. [PubMed: 16111474]
20. Arifin DR, Palmer AF. Determination of size distribution and encapsulation efficiency of liposome-encapsulated hemoglobin blood substitutes using asymmetric flow field-flow fractionation coupled with multi-angle static light scattering. Biotechnol. Prog 2003;19:1798–1811. [PubMed: 14656159]
21. Arifin DR, Palmer AF. Polymersome encapsulated hemoglobin: a novel type of oxygen carrier. Biomacromolecules 2005;6:2172–2181. [PubMed: 16004460]
22. Arifin DR, Palmer AF. Physical properties and stability mechanisms of poly(ethylene glycol) conjugated liposome encapsulated hemoglobin dispersions. Artif. Cells, Blood Substitutes Biotechnol 2005;33:137–162.
23. Arifin DR, Palmer AF. Stability of liposome encapsulated hemoglobin dispersions. Artif. Cells, Blood Substitutes Biotechnol 2005;33:113–136.
24. Li S, Palmer AF. Structure and mechanical response of self-Assembled poly(butadiene)-b-poly (ethylene oxide) colloids probed by atomic force microscopy. Macromolecules 2005;38:5686–5698.
25. Zhao J, Liu C-S, Yuan Y, Tao X-Y, Shan X-Q, Sheng Y, Wu F. Preparation of hemoglobin-loaded nano-sized particles with porous structure as oxygen carriers. Biomaterials 2007;28:1414–1422. [PubMed: 17126898]

26. Salimi A, Hallaj R, Soltanian S. Immobilization of hemoglobin on electrodeposited cobalt-oxide nanoparticles: Direct voltammetry and electrocatalytic activity. Biophys. Chem 2007;130:122–131. [PubMed: 17825977]
27. Patton JN, Palmer AF. Photopolymerization of bovine hemoglobin entrapped nanoscale hydrogel particles within liposomal reactors for use as an artificial blood substitute. Biomacromolecules 2005;6:414–424. [PubMed: 15638547]
28. Miranda JJL, Maillett DH, Soman J, Olson JS. Thermoglobin, oxygen-avid hemoglobin in a bacterial hyperthermophile. J. Biol. Chem 2005;280:36754–36761. [PubMed: 16135523]
29. Hargrove MS, Whitaker T, Olson JS, Vali RJ, Mathews AJ. Quaternary structure regulates hemin dissociation from human hemoglobin. J. Biol. Chem 1997;272:17385–17389. [PubMed: 9211878]
30. Dwek RA. Glycobiology: toward understanding the function of sugars. Chem. Rev 1996;96:683–720. [PubMed: 11848770]
31. Higgins PJ, Bunn HF. Kinetic analysis of the nonenzymic glycosylation of hemoglobin. J. Biol. Chem 1981;256:5204–5208. [PubMed: 7228877]
32. Haney DN, Bunn HF. Glycosylation of hemoglobin *in vitro*: affinity labeling of hemoglobin by glucose-6-phosphate. Proc. Nat. Acad. Sci. U.S. A 1976;73:3534–3538.
33. Tam S-C, Blumenstein J, Wong JT-F. Soluble dextran-hemoglobin complex as a potential blood substitute. Proc. Nat. Acad. Sci. U.S. A 1976;73:2128–2131.
34. Ali AC, Campbell JA. Interference of *O*-raffinose cross-linked hemoglobin with routine Hitachi 717 assays. Clin. Chem 1997;43:1794–1796. [PubMed: 9299984]
35. Adamson JG, Moore C. Hemolink, an *O*-raffinose crosslinked hemoglobin-based oxygen carrier. Blood Substit 1998;2:62–81.
36. Boykins RA, Buehler PW, Jia Y, Venable R, Alayash AI. *O*-raffinose crosslinked hemoglobin lacks site-specific chemistry in the central cavity: structural and functional consequences of β93Cys modification. Proteins: Struct. Funct. Bioinf 2005;59:840–855.
37. Baldwin AL, Wiley EB, Alayash AI. Differential effects of sodium selenite in reducing tissue damage caused by three hemoglobin-based oxygen carriers. J. Appl. Physiol 2004;96:893–903. [PubMed: 14555684]
38. Davis BG. Synthesis of glycoproteins. Chem. Rev 2002;102:579–601. [PubMed: 11841255]
39. Vasquez GB, Karavitis M, Ji X, Pechik I, Brinigar WS, Gilliland GL, Fronticelli C. Cysteines beta93 and beta112 as probes of conformational and functional events at the human hemoglobin subunit interfaces. Biophys. J 1999;76:88–97. [PubMed: 9876125]
40. Cheng Y, Shen T-J, Simplaceanu V, Ho C. Ligand binding properties and structural studies of recombinant and chemically modified hemoglobins altered at β93 cysteine. Biochemistry 2002;41:11901–11913. [PubMed: 12269835]
41. Khan I, Dantsker D, Samuni U, Friedman AJ, Bonaventura C, Manjula B, Acharya SA, Friedman JM. β93 Modified hemoglobin: kinetic and conformational consequences. Biochemistry 2001;40:7581–7592. [PubMed: 11412112]
42. Dimino ML, Palmer AF. Purification of bovine hemoglobin via fast performance liquid chromatography. J. Chromatogr. B Anal. Technol. Biomed. Life Sci 2007;856:353–357.
43. Sun G, Palmer AF. Preparation of ultrapure bovine and human hemoglobin by anion exchange chromatography. J. Chromatogr. B Anal. Technol. Biomed. Life Sci 2008;867:1–7.
44. Eike JH, Palmer AF. Effect of glutaraldehyde concentration on the physical properties of polymerized hemoglobin-based oxygen carriers. Biotechnol. Prog 2004;20:1225–1232. [PubMed: 15296452]
45. Russell WK, Park Z-Y, Russell DH. Proteolysis in mixed organic-aqueous solvent systems: applications for peptide mass mapping using mass spectrometry. Anal. Chem 2001;73:2682–2685. [PubMed: 11403317]
46. Xu H, Zhang L, Freitas MA. Identification and characterization of disulfide bonds in proteins and peptides from tandem MS data by use of the MassMatrix MS/MS search engine. J. Proteome Res 2008;7:138–144. [PubMed: 18072732]
47. Chayen NE. The role of oil in macromolecular crystallization. Structure 1997;5:1269–1274. [PubMed: 9351804]

48. Pflugrath JW. The finer things in X-ray diffraction data collection. Acta Crystallogr. Sect. D: Biol. Crystallogr 1999;D55:1718–1725. [PubMed: 10531521]

49. Mueser TC, Rogers PH, Arnone A. Interface sliding as illustrated by the multiple quaternary structures of liganded hemoglobin. Biochemistry 2000;39:15353–15364. [PubMed: 11112521]

50. Navaza J. On the computation of structure factors by FFT techniques. Acta Crystallogr. Sect. A: Found. Crystallogr 2002;A58:568–573.

51. Murshudov GN, Vagin AA, Dodson EJ. Refinement of macromolecular structures by the maximum-likelihood method. Acta Crystallogr. Sect. D: Biol. Crystallogr 1997;D53:240–255. [PubMed: 15299926]

52. Emsley P, Cowtan K. Coot: model-building tools for molecular graphics. Acta Crystallogr. Sect. D: Biol. Crystallogr 2004;D60:2126–2132. [PubMed: 15572765]

53. Engh RA, Huber R. Accurate bond and angle parameters for x-ray protein structure refinement. Acta Crystallogr. Sect. A: Found. Crystallogr 1991;A47:392–400.

54. Laskowski RA, MacArthur MW, Moss DS, Thornton JM. PROCHECK: a program to check the stereochemical quality of protein structures. J. Appl. Crystallogr 1993;26:283–291.

55. Ramachandran GN, Sasisekharan V. Conformation of polypeptides and proteins. Adv. Protein Chem 1968;23:283–438. [PubMed: 4882249]

56. Zimm BH. The scattering of light and the radial distribution function of high-polymer solutions. J. Chem. Phys 1948;16:1093–1099.

57. Biringer RG, Amato H, Harrington MG, Fonteh AN, Riggins JN, Huhmer AFR. Enhanced sequence coverage of proteins in human cerebrospinal fluid using multiple enzymatic digestion and linear ion trap LC-MS/MS. Brief. Funct. Genomics Proteomics 2006;5:144–153.

58. Pearson WR, Lipman DJ. Improved tools for biological sequence comparison. Proc. Nat. Acad. Sci. U.S. A 1988;85:2444–2448.

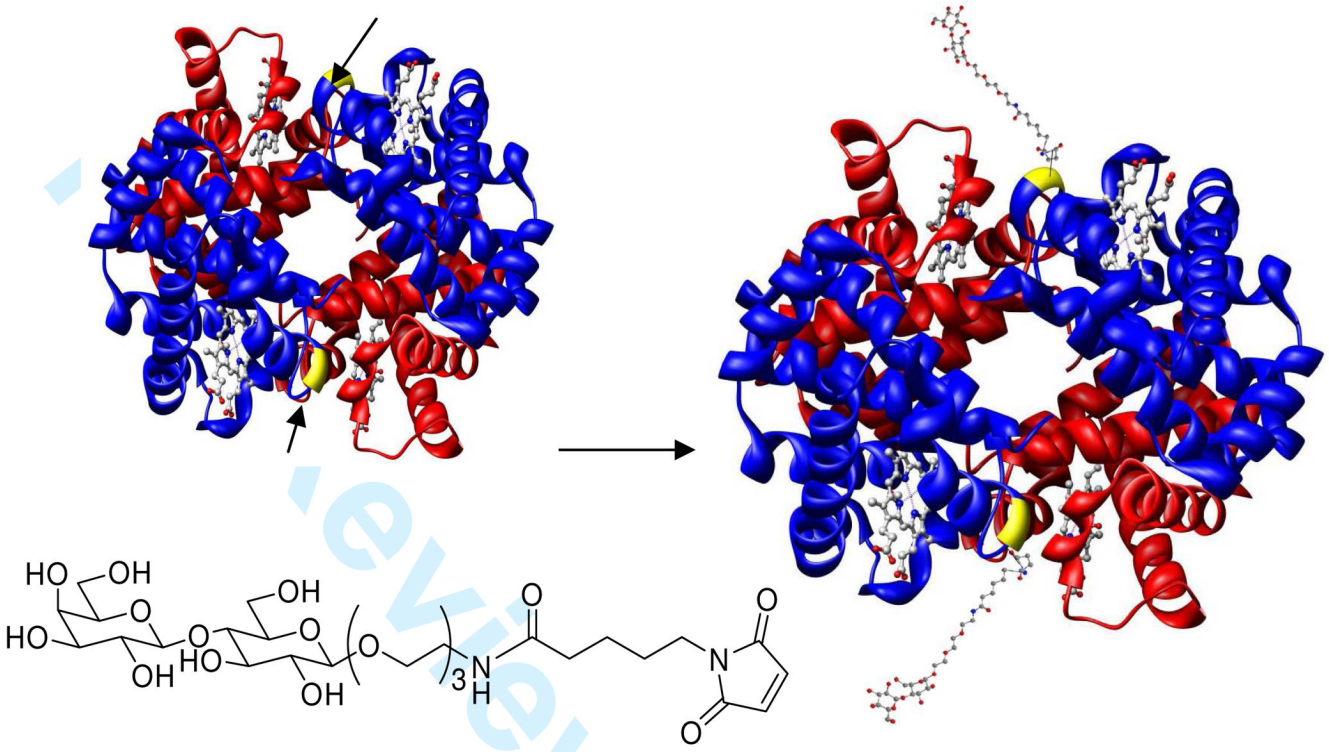

Figure 1.
Site-selective glycosylation of bovine Hb at Cys β93 by the lactose derivative.

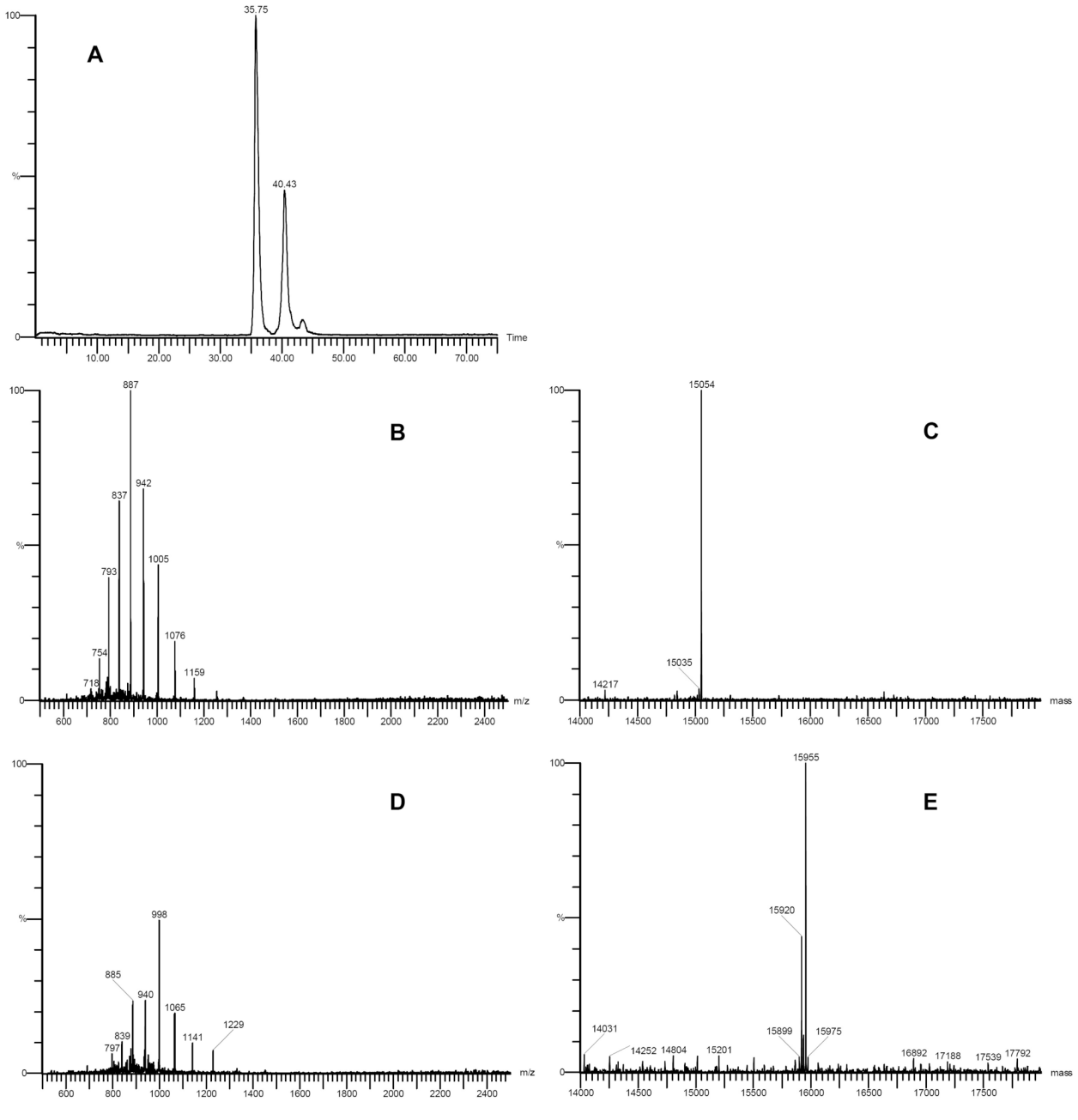

Figure 2.

Analysis of bovine Hb by LC-MS. **A** represents the RP-HPLC chromatogram of bovine Hb. **B** represents the ESI-TOF mass spectra of the peak eluting at 36.75 min. **C** represents the deconvoluted molecular ion of the peak eluting at 36.75 min. **D** represents the ESI-TOF mass spectra of the peak eluting at 40.43 min. **E** represents the deconvoluted molecular ion of the peak eluting at 40.43 min.

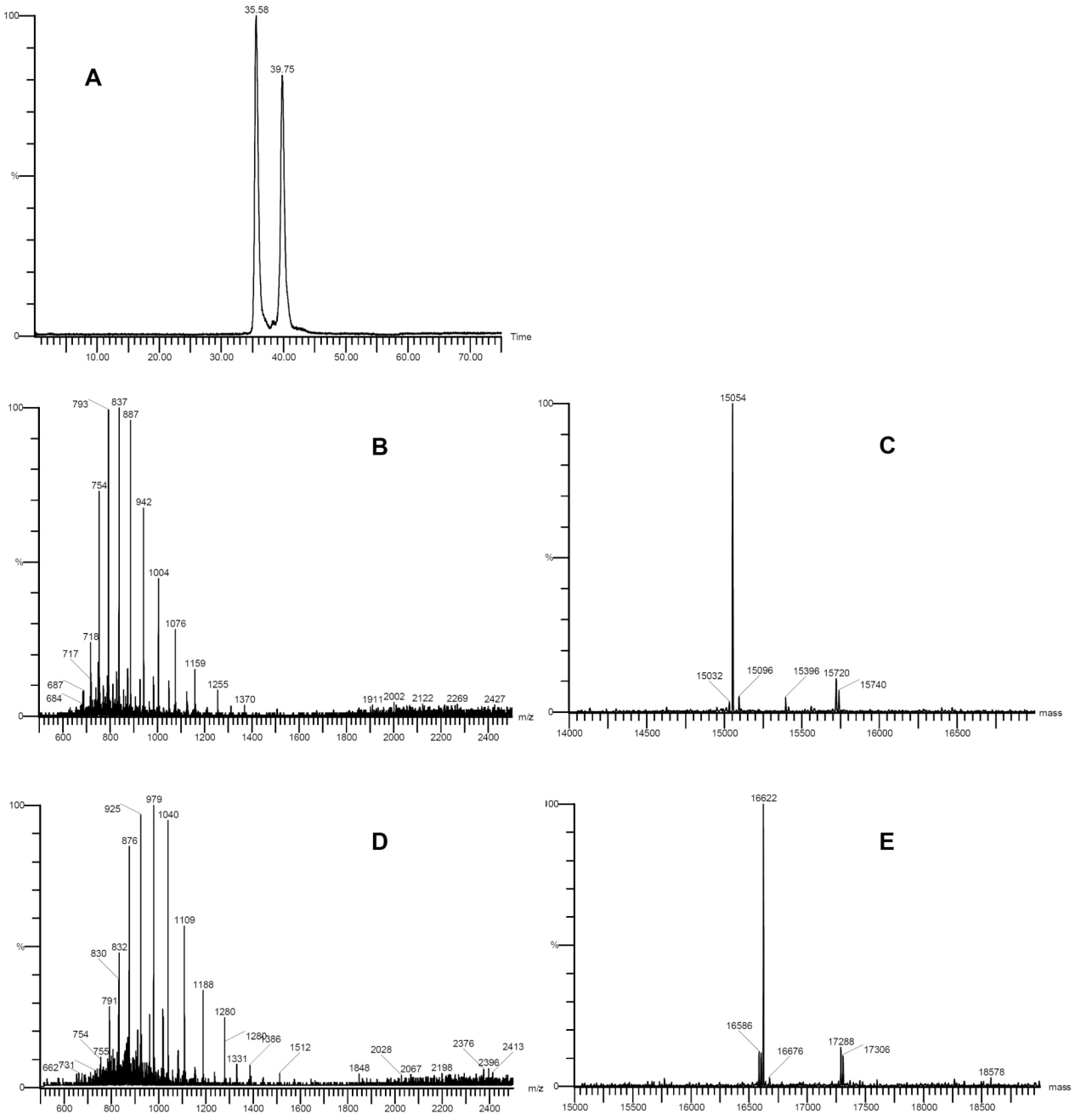

Figure 3.

Analysis of glycosylated bovine Hb by LC-MS. **A** represents the RP-HPLC chromatogram of glycosylated bovine Hb. **B** represents the ESI-TOF mass spectrum of the peak eluting at 35.58 min. **C** represents the deconvoluted molecular ion of the peak eluting at 35.58 min. **D** represents the ESI-TOF mass spectrum of the peak eluting at 39.75 min. **E** represents the deconvoluted molecular ion of the peak eluting at 39.75 min.

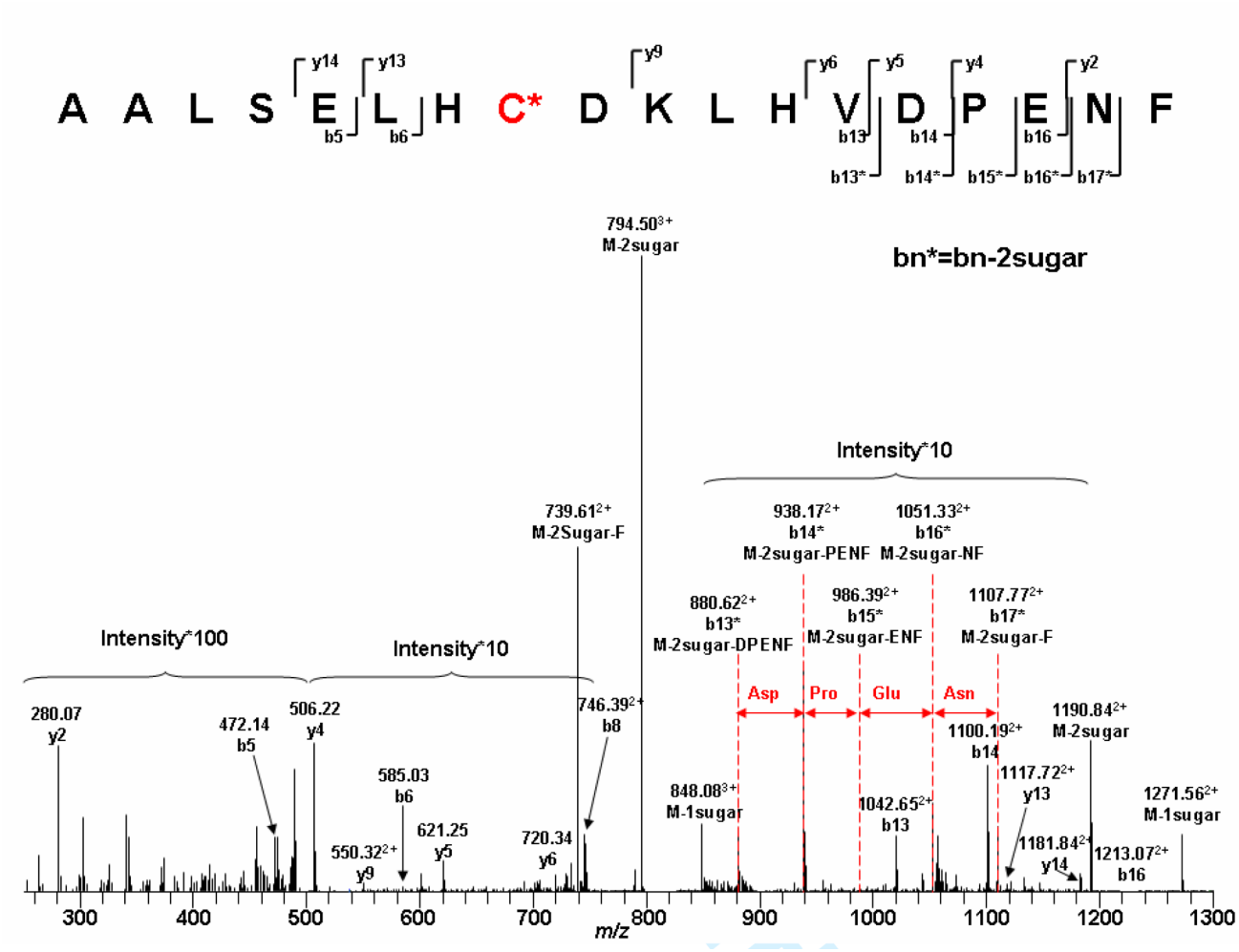

Figure 4.
ESI-MS/MS spectra of the glycosylated β-globin chymotryptic peptides 85–102. * Represents the fragment containing the lactoside derivative.

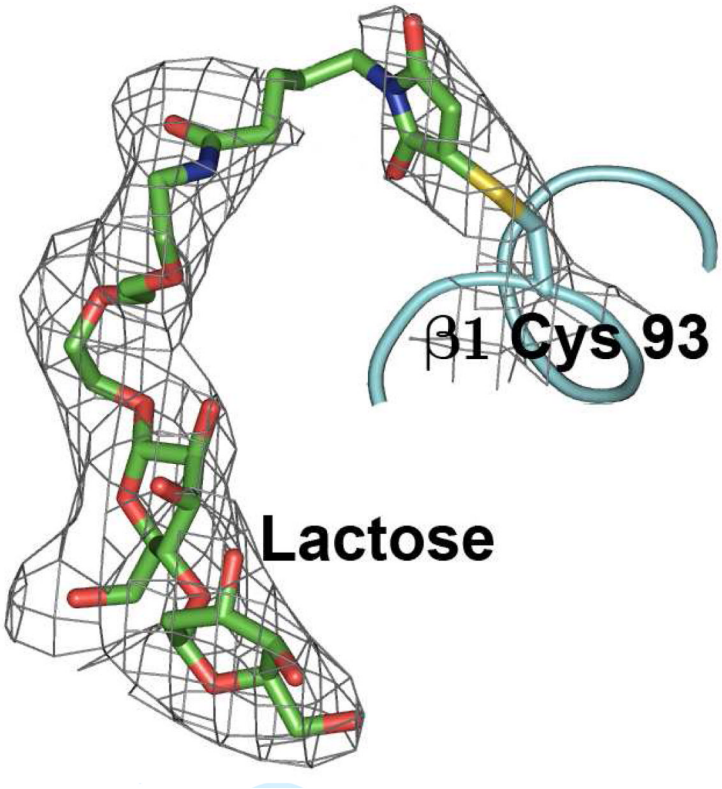

Figure 5.
Succinimide linked lactose sandwiched between the β_1 and α_2 subunits of bovine Hb.

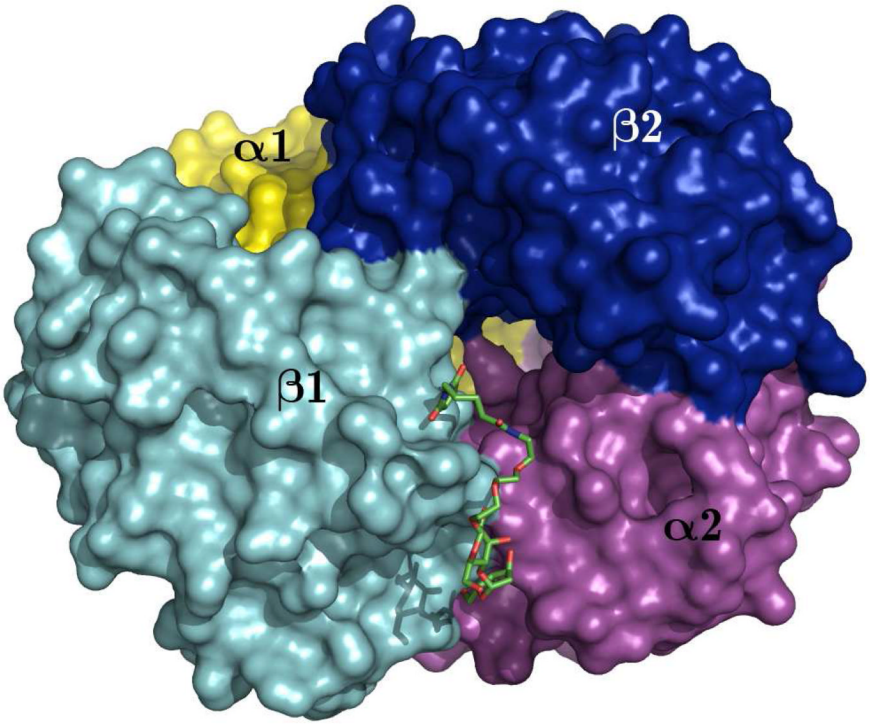

Figure 6.
Final electron density map ($2F_o$ - F_c) at 0.7σ showing β_1-Cys 93 covalently bound to the succinimide linked lactose.

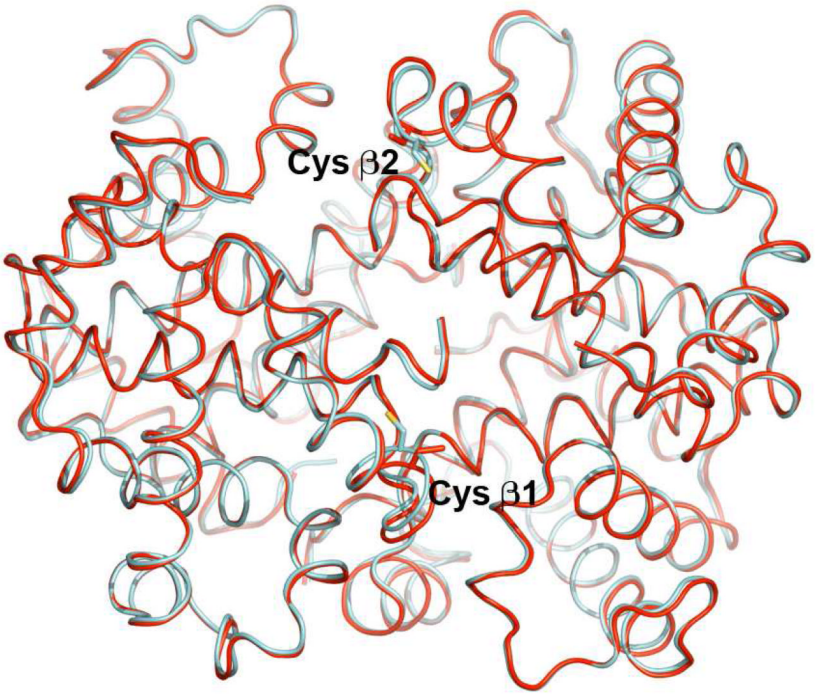

Figure 7.
Superimposition of glycosylated bovine Hb (red) and native bovine Hb (blue).

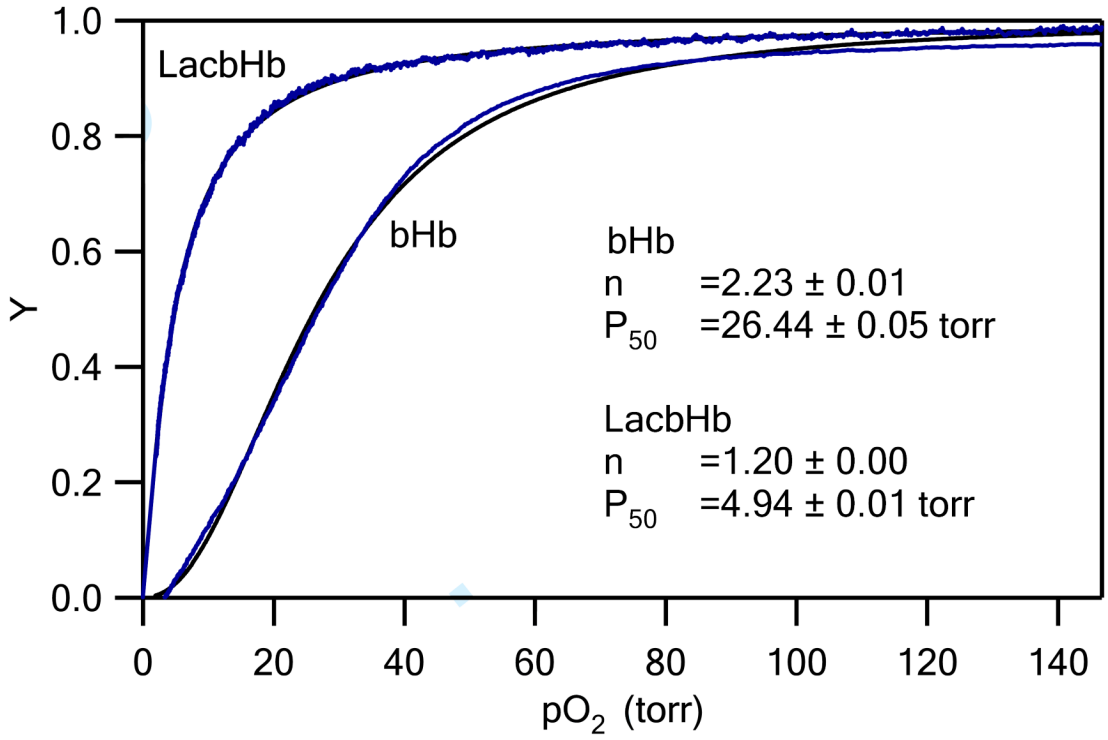

Figure 8.
Oxygen dissociation curves of bovine Hb and glycosylated bovine Hb.

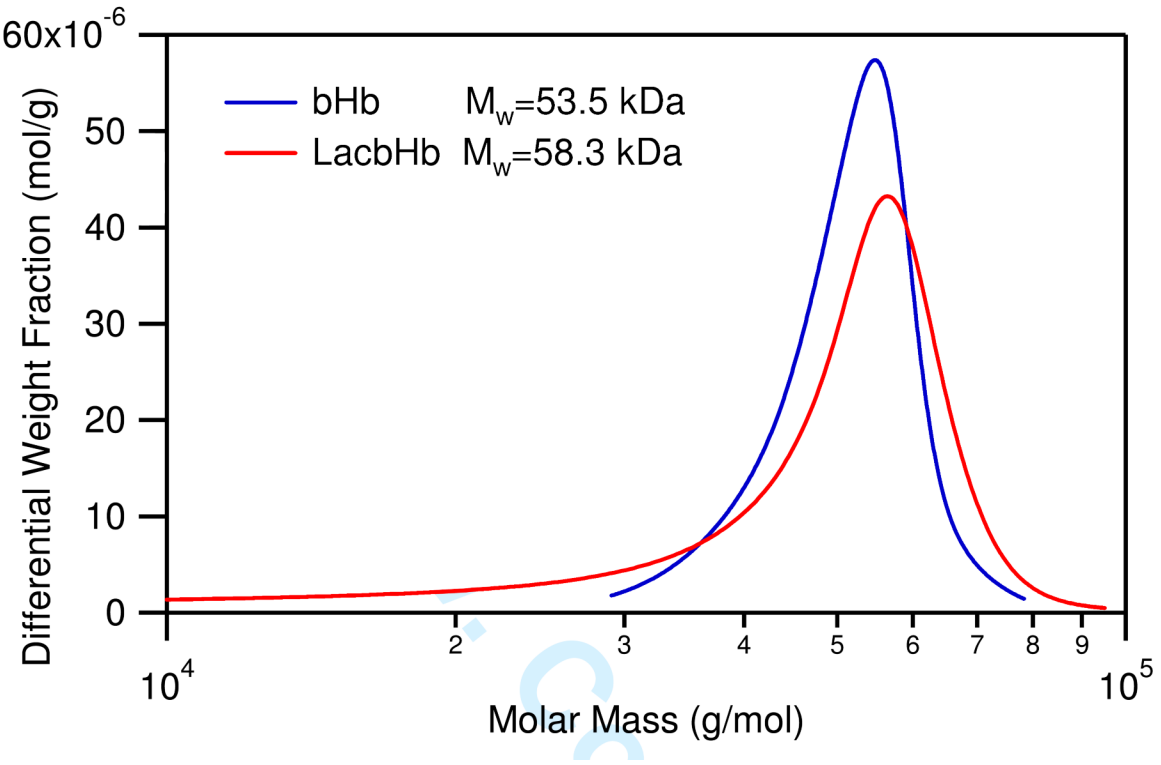

Figure 9.
Differential molar mass distribution of bovine Hb (bHb, blue) and lactoside derivative conjugated to bovine Hb (LacbHb, red).

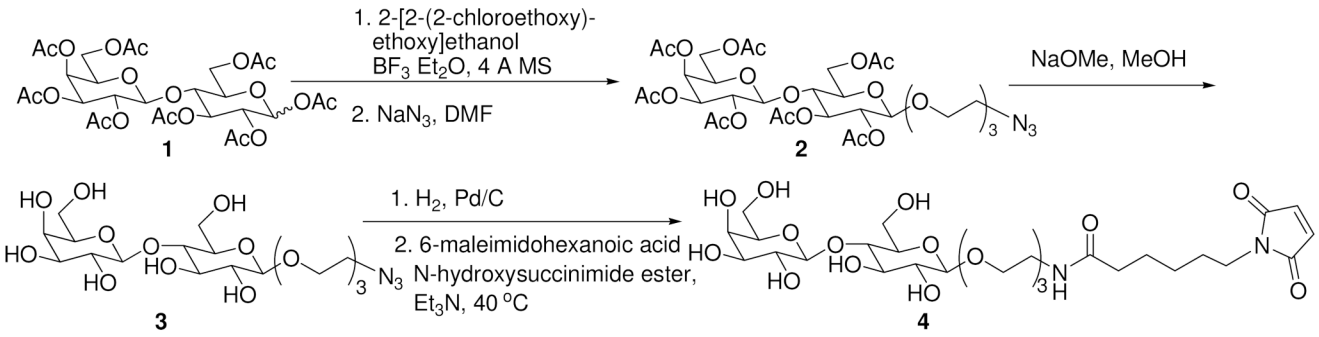

Scheme 1.
Synthesis of maleimide-lactoside for glycosylation of bovine Hb.